J Low Temp Phys (2011) 163: 370–379
DOI 10.1007/s10909-011-0355-z

Improvement of High T_c Phase Formation in *BPSCCO* Superconductor by Adding Vanadium and Substituting Titanium

Duygu Yazıcı · Bekir Özçelik · M. Eyyüphan Yakıncı

Received: 22 September 2010 / Accepted: 20 February 2011 / Published online: 11 March 2011

Abstract We have produced the $(BiPb)_2V_xSr_2Ca_3Cu_{4-y}Ti_yO_{12+\delta}$ with $x = 0.1$ and $y = 0.050, 0.10, 0.2$ and 0.3 compounds by melt-quenching method. Structural and superconducting properties of the produced samples were investigated by Scanning Electron Microscopy, X-ray diffraction patterns, electrical resistance measurements and dc-magnetic hysteresis loop measurements. The pure high-T_c phase (2223) is nearly found with Ti substitution for $x = 0.05$ and 0.10. The onset critical temperature ($T_{c\cdot onset}$) of the samples increases up to 111 K with doping up to $x = 0.20$. In addition, considerable large values of the critical current densities (J_c), calculated from the hysteresis loop measurements by using Bean's critical state model are obtained for the samples in the same doping range. Our data have indicated that J_c decreases with increasing temperature and Ti concentration.

Keywords Bi-based cuprates · XRD · Critical currents · Magnetic properties

1 Introduction

Since the discovery of BSCCO high-T_c superconductors [1], there has been tremendous effort to improve formation and stability of the (2223) phase (see for example [2]). It is well known that three phases have been established in the BSCCO superconductor with an ideal structural formula $Bi_2Sr_2Ca_{n-1}Cu_nO_{4+2n}$ where n represents the number of the CuO_2 layers in the unit cell. In all high-T_c ceramic superconductors, the CuO_2 planes which contain magnetic Cu^{2+} ions are supposed to

D. Yazıcı · B. Özçelik (✉)
Department of Physics, Faculty of Sciences and Letters, Çukurova University, 01330 Adana, Turkey
e-mail: ozcelik@cu.edu.tr

M.E. Yakıncı
Department of Physics, Faculty of Sciences and Letters, İnönü University, 44069 Malatya, Turkey

enhance the superconductivity [3]. Weak coupling between BiO-BiO layers in the BSCCO system enables the substitution of the different oxides for Bi^{3+} site. Some of the results have demonstrated that there is no significant increase in the T_c. But, important changes occur in the carrier concentration due to different cation doping levels. Therefore, the electrical property of the system varies. Here we should state that the preparation technique of a system is also very important. To this end, preparing the BSCCO system by the melt quenching technique yields good density and minimum porosity, compared to the conventional solid state technique [4–7].

The formation of pure and textured (2223) phase is a critical issue in fabricating BSCCO superconductors. Since the reaction kinetics of the Bi-(2223) phase formation is very slow, long periods of sintering at temperatures close to its decomposition temperature are required [8–10]. Many factors, including composition, phase assemblage of the precursor powder, lead content, grain alignment, intergrain connectivity, density of the core, sintering parameters and doped ions, significantly influence the heat treatment parameters and final physical properties of the samples [11]. T_c of superconducting copper-oxide based compounds depends on the density of the mobile holes in the CuO_2 planes and thus on the average Cu valency [12]. The replacement of Ca sites by rare-earth ions leads to a decrease of the formal Cu valency [13, 14], whereas, the substitution of Pb^{2+} in Bi^{3+} site increases Cu valency [15]. However, the value of the transition temperature can further be increased either by quenching or by annealing under reduced pressures (vacuum or nitrogen), because T_c shows a strong dependence on the preparation conditions.

As stated in the previous paragraph it has now been well established that the superconducting properties of the copper oxide superconductors are related to the hole concentration. Nevertheless, there are few reports on the effects of substitutions to Cu site by other valence cations like Fe, Co, Cr in the BSCCO (2223) system [16–20]. It was obtained that partial Sr substitution by Ba leads to an increase of $T_{c.onset}$ and to a decrease of the modulation period [19].

As it is mentioned above much effort has been devoted to form the (2223) phase by changing the nominal composition of some elements. The (2223) phase has a tendency to decompose to low-T_c (2212) and (2201) phases at certain temperatures. Therefore, this makes more difficult to understand complicated mechanism involved in the (2223) formation process. It was obtained that partial substitution of trivalent Bi with Pb has stabilized the (2223) phase and the nominal concentration of Pb was determined as 0.4 [21, 22]. On the other hand it is also reported that nearly no change at $T_{c.onset}$ and a broadening of the superconducting transitions together with an increase of low-T_c (2212) and (2201) phase [20]. Since crystal structures of (2212) and (2223) are very similar, it often results in intergrowth of these phases in the material.

In a recent study, it is reported that Nb addition increases considerably formation of the (2223) phase, up to 96% [23]. In this study, our purpose is to synthesize the samples in which high-T_c (2223) phase is highly formed. To our best of knowledge some other high valency cations, like Nb, will make the similar effect. For this reason, we will investigate the appropriate cations and substitute them with Bi and Cu-sites independently and observe formation of the (2223) phase variation.

2 Experimental Process

The appropriate amounts of Bi_2O_3, PbO, TiO_2, V_2O_5, $SrCO_3$, $CaCO_3$, and CuO fine powders in the stoichiometric ratios of $Bi_{1.6}Pb_{0.4}V_xSr_2Ca_3Cu_{4-y}Ti_yO_{12+\delta}$ ($x = 0.1$ and $y = 0.05, 0.1, 0.2,$ and 0.3) were well mixed by milling and calcined at 750°C for 24 h in air. The mixture was re-ground for about one-half hours and the resulting powder was placed in a platinum crucible and heated at 1200°C until the samples were completely melted. The melts were poured onto a pre-cooled copper plate and pressed quickly by another copper plate to obtain an approximately 1.5 to 2 mm thick plate like amorphous (glass) material. The mixture was re-ground for about two hours and the resulting powder were then pressed into pellets of 13 mm diameter by applying a 5 tons pressure. Finally, the precursor materials produced were annealed at 845°C for 185 h in air to achieve crystallized material and superconductivity. The samples with $x = 0.1$ and $y = 0.050, 0.10, 0.2$ and 0.3 will be hereafter named as A, B, C, and D, respectively.

Resistivity measurements were carried out on our samples using a standard four-probe method with silver paint contact. X-ray powder diffraction analyses were performed by using Rigaku RadB powder diffractometer system with CuKα radiation and a constant scan rate between $2\theta = 3$–60° at room temperature, to examine the phases present in the samples. SEM photographs for the study of the microstructure were taken by using a LEO Evo-40 VPX scanning electron microscope (SEM) and Röntec energy dispersive X-ray spectroscopy (EDX). The magnetic measurements were performed with a 7304 model Lake Shore VSM.

3 Results and Discussions

The normalized resistance to room temperature of the samples is presented in Fig. 1. For the samples A and B although the $T_{c.onset}$'s (below which the sample is in a superconducting state) of superconductivity are about 111 K, R almost goes to zero at $T_{c.offset} = 101$ K. Hence, there is a superconducting transition range ΔT of about 10 K, this means that the high-T_c phase (2223) is the dominant phase in the samples. We should emphasize here that the sample A appears to have the best formation of the

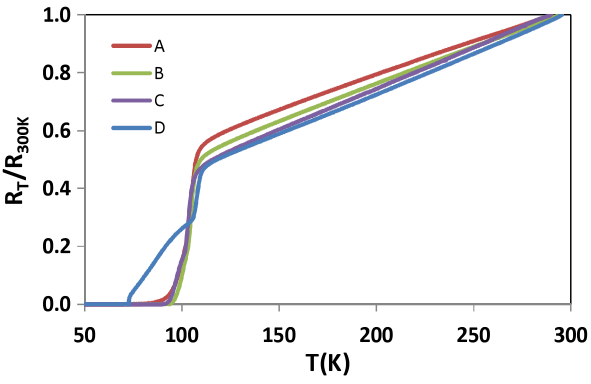

Fig. 1 (Color online) Temperature dependence of resistivity for the samples A, B, C, and D

Table 1 The T_c's values deduced from R-T data

Sample	T_c (K)
A	$T_{c.onset} = 111.76$ $T_{c.offset} = 101.34$
B	$T_{c.onset} = 110.30$ $T_{c.offset} = 101.84$
C	$T_{c.onset} = 109.65$ $T_{c.offset} = 94.60$
D	$T_{c.onset} = 111.64$ $T_{c.offset} = 72.38$

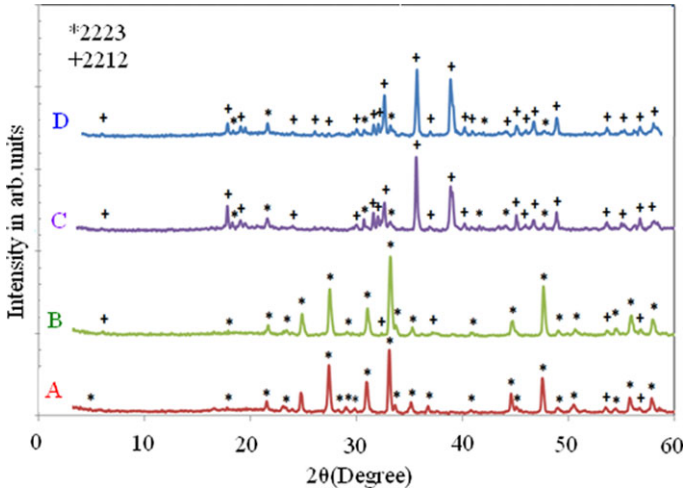

Fig. 2 (Color online) XRD patterns of (*a*) A , (*b*) B (*c*) C and (*d*) D samples

(2223) phase. On the other hand, for the samples C and D further increase in Ti concentration causes a broadening transition and a decrease of the $T_{c.offset}$ values. This behavior indicates that increasing the amount of Ti, necessarily favors the formation of the (2212) phase instead of the common (2223) phase. The steady decreases in the resistance of each sample down to ≈110 K can be explained by the metallic character of the samples. As a result our resistance measurements have shown that the (2223) phase is dominant both for the samples A and B.

The deduced $T_{c.onset}$'s and $T_{c.offset}$'s values from *R-T* measurements are tabulated in Table 1 for the samples A, B, C and D.

The XRD diffraction patterns of A, B, C and D samples are shown in Fig. 2. It is shown that, the (2223) phase is highly formed for A and B samples. The other unwanted peaks in the XRD pattern are diminishingly small. This reveals that sufficient reaction at the melt interface has resulted in an almost pure high-T_c phase sample. As a result, with increasing Ti concentration in the system, the (2223) phase is nearly single (97%) in the A sample. One should emphasize here that the resistance mea-

Table 2 Unit cell parameters, high and low-T_c phase fractions of Ti doped samples

Sample	2223 (%)	2212 (%)	$a = b$ (Å)	c(Å)
A	97	3	5.4037	37.0192
B	87	13	5.4031	36.9931
C	30	70	5.4067	30.7459
D	5	95	5.4039	30.7198

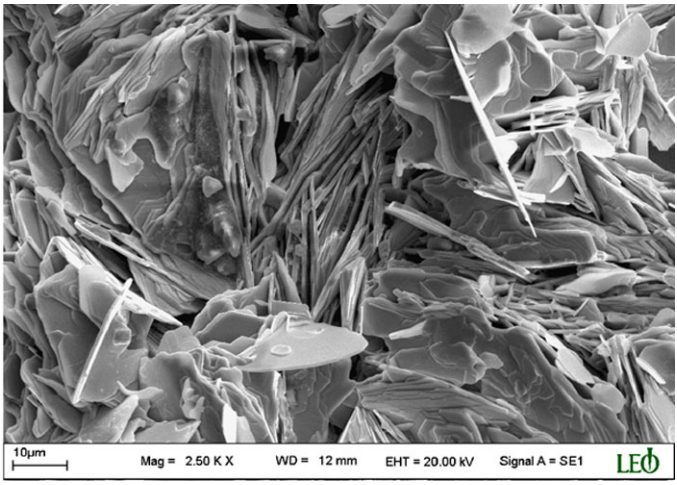

Sample A

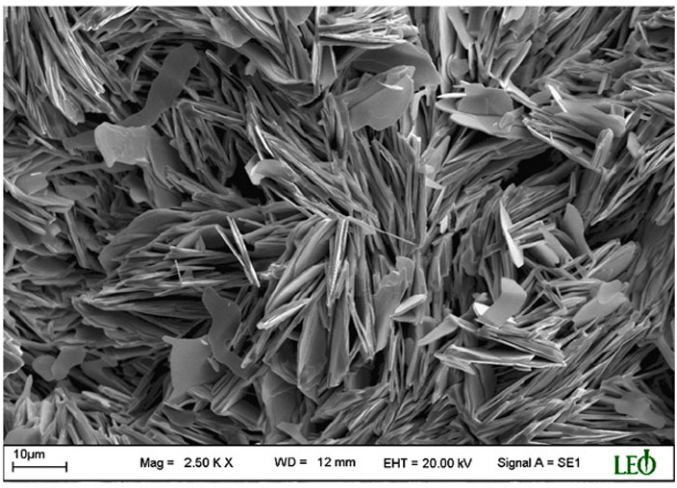

Sample B

Fig. 3 (Color online) SEM photographs of the samples

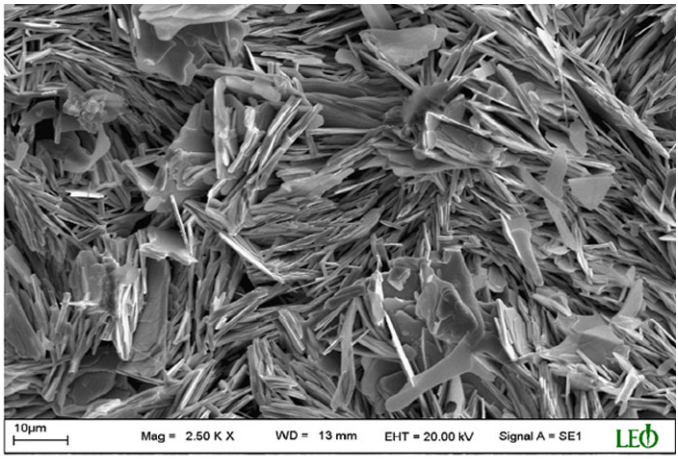

Sample C

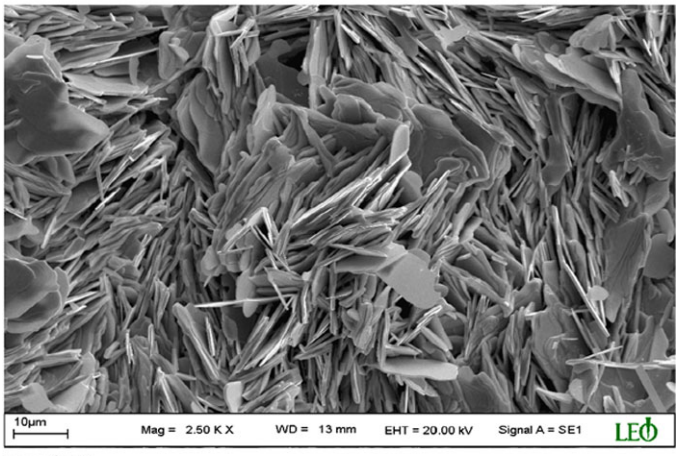

Sample D

Fig. 3 (*Continued*)

surement of sample D demonstrates a very broad transition with a width of about 40 K. In our opinion, this may be due to the coexistence of low T_c phases (2201) in very low percentages which could not be detected in the XRD analysis.

Unit cell parameters and high and low-T_c phase fractions of Ti doped samples are presented in Table 2.

The SEM photographs are illustrated in Fig. 3 for the different Ti doped samples. All the figures contain both needle shapes and grain structure. This supports our resistivity and XRD results which show that the (2223) phase is the dominant phase in our samples. The samples A and B have a more uniform surface with a dense alignment of grains and needle shape. It is seen that surface composition of the samples A and B is closer to that of the Bi-(2223) phase. This is also confirmed by the XRD and resistivity measurements given above. By using the experimental results given above, it

Table 3 J_{cmag} result of samples A, B, C, and D

Sample	J_{cmag} (A/cm^2) 9 K	J_{cmag} (A/cm^2) 15 K	J_{cmag} (A/cm^2) 20 K	J_{cmag} (A/cm^2) 25 K
A	1.4×10^5	0.73×10^5	0.49×10^5	0.28×10^5
B	0.85×10^5	0.54×10^5	0.43×10^5	0.18×10^5
C	0.65×10^5	0.45×10^5	0.28×10^5	0.14×10^5
D	0.58×10^5	0.39×10^5	0.23×10^5	0.11×10^5

is possible to conclude that our samples have both high-T_c (2223) and low-T_c (2212) phases, with the fraction of latter being higher for the samples C and D. This is an evidence of inhomogeneous distribution of the two phases in these samples.

The magnetic hysteresis cycles (M–H) of the compounds were performed between the fields of ±5 kOe for four different temperatures, 9, 15, 20 and 25 K. All those M–H hysteresis loops were obtained after cooling the sample in zero magnetic field (ZFC). Typical examples of magnetic hysteresis loops for the samples A and D obtained are presented in Figs. 4 and 5 respectively. It is possible to state that the superconducting properties of the sample A are much better than that of the others, since its hysteresis loop is much larger. We note the fast decrease of hysteresis loops with increasing temperature and the symmetrical behavior. Thus we may suggest that the magnetization behaviors at low fields are dominated by the bulk pinning rather than surface and geometrical barriers [12]. As can be seen from these figures, due to the pinning effects and large volume of the superconducting regions, the field penetration becomes difficult below 9 K, but the applied fields begin to significantly penetrate into the samples at higher temperatures due to the decrease in superconducting regions with increasing temperature. This is probably the reason for large decreases appearing in the width of the magnetic hysteresis loops above 9 K.

The J_{cmag} values of the samples were calculated using the Bean's model [24];

$$J_{cmag} = 20\frac{\Delta M}{a(1 - a/3b)}$$

where, J_{cmag} is the magnetization current density in amperes per square centimeter of a sample. $\Delta M = M_+ - M_-$ is measured in electromagnetic units per cubic centimeter, a and $b(a < b)$ are the dimensions in centimeters of the cross-section of the sample parallel to the applied field.

Figures 6 and 7 show the calculated critical current densities of the samples as a function of the applied field, at for four different fixed temperatures. As can be seen from Fig. 6 and Table 3, the maximum value of J_c, at 9 K, is calculated as 1.4×10^5 A/cm^2 for sample A, and then decreases with increasing temperature. All the samples prepared show that the field dependence of J_{cmag} is strong even at 9 K (Figs. 6 and 7). This kind of behavior can be explained in terms of weak grain connectivity and/or an increased volume fraction of impurity grains, such as formation of both BiPb-2212 and BiPb-2223 phases.

In general, higher values of J_c have been observed while weak magnetic field dependence was still obtained at $T > 9$ K. This is expected because the magnetization

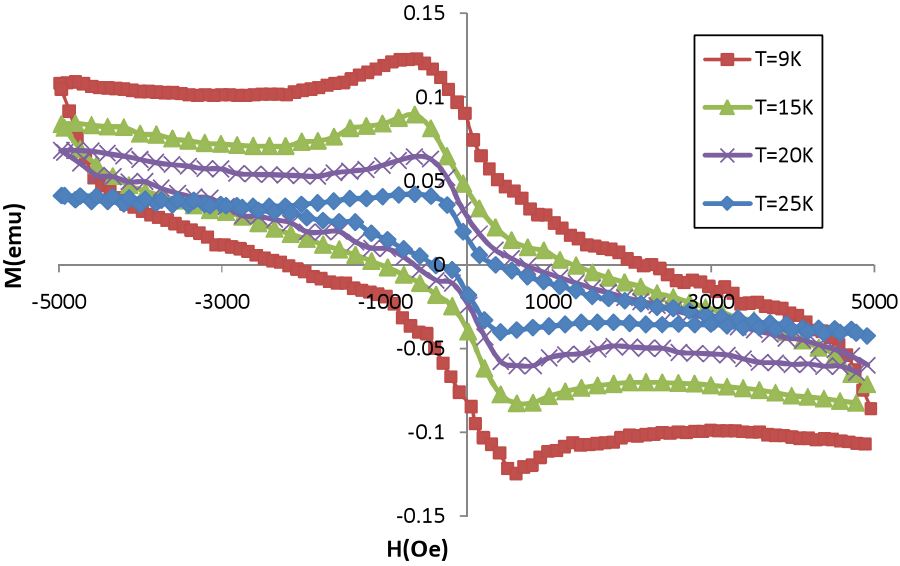

Fig. 4 (Color online) $M-H$ hysteresis of sample A

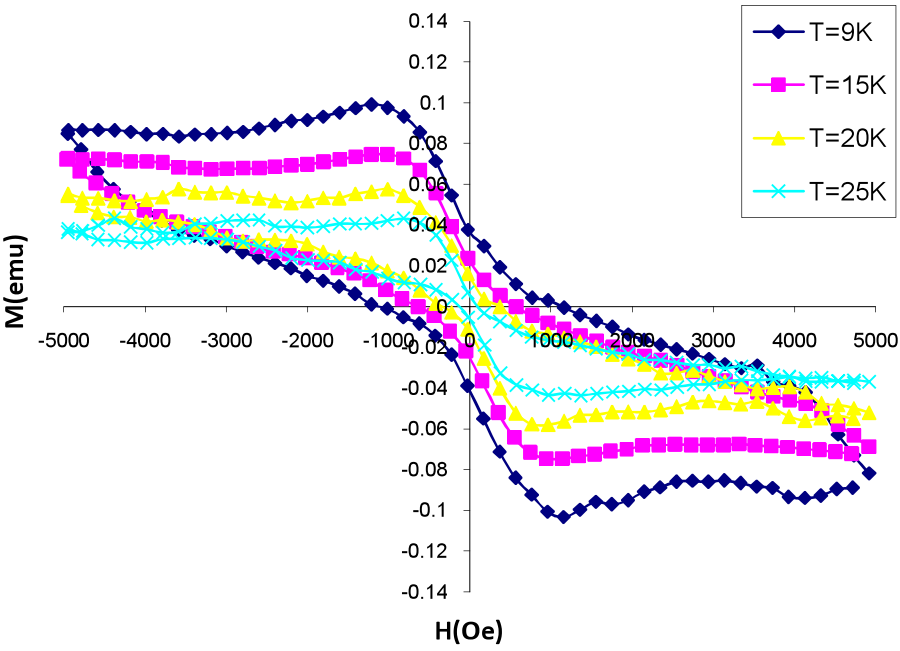

Fig. 5 (Color online) $M-H$ hysteresis of sample D

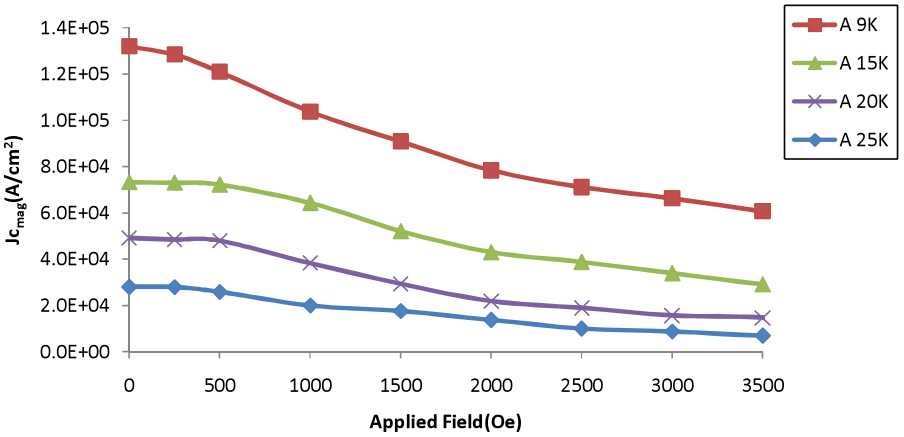

Fig. 6 (Color online) J_{cmag} results of sample A

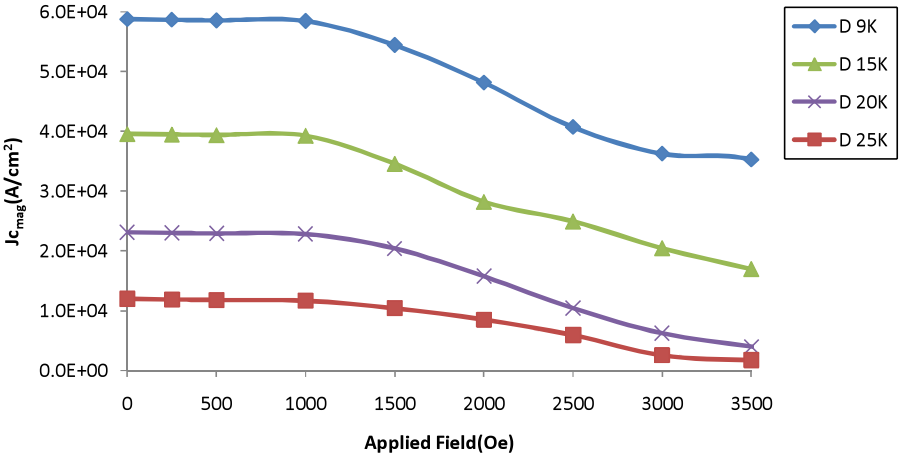

Fig. 7 (Color online) J_{cmag} result of sample D

curve of the sample forms a loop that indicates the presence of the pinning centers on the surface of the materials. It is also well known that in the high-T_{c} superconducting material, non-superconducting impurity phases are highly effective in the flux-pinning mechanism. Thus, a higher critical current density with small amount of non-superconducting phases is possible the result of pinning mechanism in the superconductor.

4 Conclusion

The results presented above indicate that the adding of Vanadium in Bi-site and substituting of Titanium in Cu-site enhances the superconducting properties of the pure

(2223) phase up to $x = 0.1$ and improves the critical parameters T_c and J_c. The volume fraction of the high-T_c (2223) phase reaches 97% for the sample A with the V and Ti concentration of 0.1 and 0.05, respectively. Therefore it is possible to argue that transition ions appear to play an important role for the enhancement of superconducting properties.

Acknowledgement This work is supported by Research Fund of Çukurova University, Adana, Turkey, under grant contracts no: FEF2009D11.

References

1. H. Maeda, Y. Tanaka, M. Fukotomi, T. Asano, Jpn. J. Appl. Phys. **27**, 209 (1988)
2. H. Maeda, K. Togana (eds.), *Bismuth-based High-Temperature Superconductors* (Marcel Dekker, New York, 1996)
3. P.W. Anderson, Science **235**, 1196 (1987)
4. A. Ekicibil, A. Coşkun, B. Özçelik, K. Kiymaç, Mod. Phys. Lett. B **18**(23), 1 (2004)
5. M.A. Aksan, M.E. Yakıncı, Y. Balcı, J. Supercond. **15**(6), 553 (2002)
6. M.E. Yakıncı, J. Phys., Condens. Matter **9**, 1105 (1997)
7. M.A. Aksan, M.E. Yakıncı, Y. Balcı, Supercond. Sci. Technol. **13**, 955 (2000)
8. J. Jiang, J.J. Abell, Supercond. Sci. Technol. **11**, 7005 (1998)
9. B. Özkurt, A. Ekicibil, M.A. Aksan, B. Özçelik, M.E. Yakıncı, K. Kıymaç, J. Low Temp. Phys. **147**, 31 (2007)
10. B. Özkurt, A. Ekicibil, M.A. Aksan, B. Özçelik, M.E. Yakıncı, K. Kiymaç, J. Low Temp. Phys. **149**, 105 (2007)
11. J.P. Singh, J. Jou, N. Vasanthamahan, R.B. Poeppel, J. Mater. Res. **8**, 2458 (1993)
12. B. Chevalier, B. Lepine, A. Lalerzin, J. Darriet, J. Eournau, J.M. Tarascon, Mater. Sci. Eng. B **2**, 277 (1989)
13. B. Jayaram, P.C. Lanchester, M.T. Weller, Physica C **160**, 17 (1989)
14. A. Coşkun, A. Ekicibil, B. Özçelik, K. Kıymaç, Chin. Phys. Lett. **21-10**, 2041 (2004)
15. M. Kappinen, A. Fukuoka, J. Wang, S. Tanaka, M. Wakafa, T. Ikemachi, H. Yamauchi, Physica C **208**, 130 (1988)
16. G. Ilonca, A.V. Pop, C. Corega, I.I. Geru, V.G. Canter, L.A. Konopko, Y. Min, R. Deltour, Physica C **235–240**, 1391 (1994)
17. K. Yanagisawa, Y. Matsui, K. Shoda, E. Takayama-Muromachi, S. Horiuchi, Physica C **196**, 34 (1992)
18. D. Ciurcha, A.V. Pop, O. Cozar, Gh. Ilonca, V.I. Geru, V. Pop, L.A. Konopko, Supercond. Sci. Technol. **9**, 88 (1996)
19. M. Zhiguiang, F. Chenaggao, S. Lei, Y. Zhen, Y. Li, W. Yu, Phys. Rev. B **4**, 14427 (1993)
20. A. Sidorenko, E.-W. Scheidt, F. Haider, M. Klemm, S. Horn, L. Konopko, R. Tidecks, Physica B **321**, 298 (2002)
21. N. Kijima, N. Endo, J. Tsuchiya, A. Sumiyama, M. Mizino, Y. Oguri, Jpn. J. Appl. Phys. **27**, L821 (1988)
22. Y.T. Huang, R.G. Liu, S.W. Lu, P.T. Wu, W.N. Wang, Appl. Phys. Lett. **56**, 779 (1990)
23. H. Sözeri, N. Ghazanfari, H. Özkan, A. Kılıç, Supercond. Sci. Technol. **20**, 1 (2007)
24. C.P. Bean, Phys. Rev. Lett. **8**, 250 (1962)